ChemPubSoc Europe

DOI: 10.1002/chem.201602906

CHEMISTRY A European Journal Full Paper

Cooperative Effects

Structural and Mechanistic Insights into s-Block Bimetallic Catalysis: Sodium Magnesiate-Catalyzed Guanylation of Amines

Marco De Tullio,[a] Alberto Hernán-Gómez,[a] Zoe Livingstone,[a] William Clegg,[b] Alan R. Kennedy,[a] Ross W. Harrington,[b] Antonio Antiñolo,[c] Antonio Martínez,[c] Fernando Carrillo-Hermosilla,*[c] and Eva Hevia*[a]

In memory of Roberto Sanchez Delgado

Abstract: To advance the catalytic applications of s-block mixed-metal complexes, sodium magnesiate $[NaMg(CH_2SiMe_3)_3]$ (**1**) is reported as an efficient precatalyst for the guanylation of a variety of anilines and secondary amines with carbodiimides. First examples of hydrophosphination of carbodiimides by using a Mg catalyst are also described. The catalytic ability of the mixed-metal system is much greater than that of its homometallic components $[NaCH_2SiMe_3]$ and $[Mg(CH_2SiMe_3)_2]$. Stoichiometric studies suggest that magnesiate amido and guanidinate complexes are intermediates in these catalytic routes. Reactivity and kinetic studies imply that these guanylation reactions occur via (tris)amide intermediates that react with carbodiimides in insertion steps. The rate law for the guanylation of *N*,*N*′-diisopropylcarbodiimide with 4-*tert*-butylaniline catalyzed by **1** is first order with respect to [amine], [carbodiimide], and [catalyst], and the reaction shows a large kinetic isotopic effect, which is consistent with an amine-assisted rate-determining carbodiimide insertion transition state. Studies to assess the effect of sodium in these transformations denote a secondary role with little involvement in the catalytic cycle.

Introduction

Over the past decade, alkaline-earth metal catalysis has started to gain prominence and find applications for the heterofunctionalization of a wide range of unsaturated organic fragments.[1] Seminal contributions from the groups of Hill[2] and Harder,[3] among others, have added Group 2 metal complexes to the homogeneous catalytic landscape as low-toxicity, low-cost alternatives to transition-metal systems. Most initial applications have involved the hydroamination of unsaturated organic substrates, such as alkenes and alkynes, in which heavier Ca or Sr complexes have demonstrated remarkable catalytic capabilities.[4] In contrast, success with Mg has been more limited because its smaller radius raises transition-state barriers in rate-determining alkene insertion steps, which shows similar patterns to those previously observed for organolanthanide(III) catalysts.[5] To overturn this trend, we have shown recently that Mg activated within a sodium magnesiate platform can outperform Ca and Ba systems in the hydroamination of isocyanates, secure higher yields, and show superior substrate scope under milder conditions.[6] Cooperative effects between the two metals underpin this catalytic transformation,[7] in which Lewis acidic Na anchors and activates the isocyanate to enable intramolecular attack by the highly nucleophilic Lewis basic tris(amido) magnesiate, which facilitates a synergistic scenario that is not available in the aforementioned single-metal systems.

To build on these initial findings and on previous studies on alkali-metal magnesiate chemistry, which have already demonstrated the unique synergistic properties of these bimetallic systems (e.g., enhanced reactivity, special regioselectivity, excellent functional-group tolerance) in several cornerstone stoichiometric transformations,[8] here we assess the ability of sodium magnesiates to catalyze the guanylation of amines with carbodiimides (Scheme 1).

The synthesis of guanidines has received considerable attention[9] because these simple nitrogen-containing molecules are valuable building blocks present in numerous natural products and pharmaceuticals.[10] Furthermore, they find extensive applications as precursors of ancillary ligands for numerous transition-, lanthanoid-, and main-group-metal complexes[11] and

[a] *M. De Tullio, Dr. A. Hernán-Gómez, Dr. Z. Livingstone, Dr. A. R. Kennedy, Prof. E. Hevia*
WestCHEM, Department of Pure and Applied Chemistry
University of Strathclyde
295 Cathedral Street, Glasgow, G1 1XL (UK)
E-mail: eva.hevia@strath.ac.uk

[b] *Prof. W. Clegg, Dr. R. W. Harrington*
School of Chemistry
Newcastle University
Newcastle upon Tyne, NE1 7RU (UK)

[c] *Prof. A. Antiñolo, A. Martínez, Dr. F. Carrillo-Hermosilla*
Centro de Innovación en Química Avanzada (ORFEO-CINQA) Departamento de Química Inorgánica, Orgánica y Bioquímica, Facultad de Ciencias y Tecnologías Químicas, Universidad de Castilla-La Mancha Campus Universitario, 13071 Ciudad Real (Spain)
E-mail: Fernando.Carrillo@uclm.es

Supporting information and ORCID(s) from the author(s) for this article is available on the WWW under http://dx.doi.org/10.1002/chem.201602906.

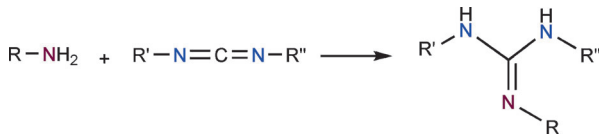

Scheme 1. Guanylation of primary amines with carbodiimides.

they can also be employed as organocatalysts.[12] Atom-economical catalytic addition of amines to carbodiimides (guanylation reaction, Scheme 1) constitutes one of the most straightforward routes to access N-substituted guanidines.[9]

Although certain guanylations can be accomplished catalyst-free, these processes have high kinetic barriers that require the use of harsh reaction conditions, which restricts their application to activated primary aliphatic amines.[13] Thus, metal catalysis is required when using anilines or secondary amines and high temperatures are needed even so, with only a select few catalytic systems able to facilitate these processes at room temperature.[9]

The vast majority of these studies have focused on transition-metal and rare-earth-metal catalysis.[14] Notwithstanding, some recent studies of lithium[15,16a] or magnesium (and heavier Group 2 elements)[16,17] have already demonstrated the potential of s-block metal complexes to catalyze these reactions. Related studies that investigated the synthesis of phosphaguanidines have revealed the ability of heavier alkaline-earth-metal amides to catalyze the direct addition of secondary phosphines to carbodiimides.[18]

With the aim of expanding the scope of s-block cooperative catalysis, here we report the first catalytic applications of alkali-metal magnesiates for the synthesis of guanidines. By combining kinetic experiments with stoichiometric reactivity studies, we provide informative mechanistic insights into these new ate-catalyzed transformations.

Results and Discussion

Catalytic synthesis of guanidines and phosphaguanidines

We began our studies by testing the efficacy of homoleptic sodium magnesiate $[NaMg(CH_2SiMe_3)_3]$ (**1**)[19] in the intermolecular hydroamination reaction of different carbodiimides with a variety of aromatic, aliphatic, and secondary cyclic amines (guanylation process). In addition, we tested compound **1** in the hydrophosphination reaction of the same carbodiimide substrates with the secondary phosphine Ph_2PH (Scheme 2).

First we studied, as a model reaction, the guanylation of 2,6-dimethylaniline **2f** with *N*,*N*′-diisopropylcarbodiimide (DIC, **3a**; Table 1) in C_6D_6 with 2 mol% of **1**. At room temperature, the reaction gave corresponding guanidine **4h** in 90% yield after 3 h. An important solvent effect was noted and when a more polar ethereal solvent with a greater coordination ability ($[D_8]$THF) was employed, guanidine **4h** was obtained in 99% yield after just 15 min. In contrast, to illustrate the synergic reactivity of **1**, when its single-metal components were tested as catalysts under the same reaction conditions, lower conversions for guanidine **4h** were observed after 15 min, with

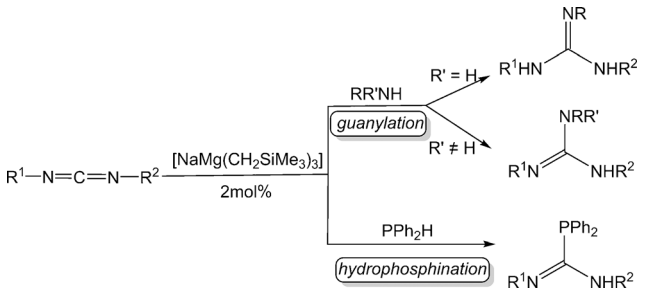

Scheme 2. Catalytic guanylation and hydrophosphination reactions.

Table 1. Optimization of the reaction conditions.

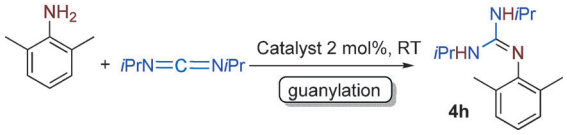

Entry	Catalyst [2 mol%]	Solvent	Time [h]	Yield [%][a]
1	$[NaCH_2SiMe_3]$	$[D_8]$THF	0.25	72
			1	84
2	$[Mg(CH_2SiMe_3)_2]$	$[D_8]$THF	0.25	44
			16	99
3	$[NaMg(CH_2SiMe_3)_3]$ (1)	$[D_8]$THF	0.25	99
4	$[NaMg(CH_2SiMe_3)_3]$ (1)	C_6D_6	3	90

[a] Yields obtained by using spectroscopic ^{1}H NMR integration of signals for the guanidine product **4h**, with addition of ferrocene (10 mol%) as the internal standard. Reaction conditions: solvent (0.5 mL), 2,6-dimethylaniline (0.55 mmol), DIC (0.5 mmol), and catalyst (0.01 mmol).

$Mg(CH_2SiMe_3)_2$ being significantly less efficient (44% conversion) than the more polar, more reactive $NaCH_2SiMe_3$ (72% conversion; Table 1). This notable influence of the metals contrasts with recent studies by Harder et al., who used a naked $\{NPh_2\}^-$ anion as an organocatalyst.[3a]

Subsequently, the catalytic activity of **1** was investigated for a range of amines and carbodiimides (Table 2, see also the Experimental Section). Aniline (**2a**) reacted with DIC (**3a**), *N*,*N*′-dicyclohexylcarbodiimide (DCC; **3b**), and EtNCN*t*Bu (**3c**), to give guanidines **4a–c** in high yields (80–96%; Table 2, entries 1–3). It is worth noting that precatalyst **1** was compatible with both electron-donating and -withdrawing substituents on the phenyl ring of the amine, such as Me-, *tert*-butyl-, MeO-, or Cl- (Table 2, entries 4–7), and gave corresponding substituted guanidines **4d–g** in excellent yields (80–98%). Furthermore, **1** also effectively facilitated the room-temperature addition of hindered anilines with substituents at their *ortho*-positions (**2f–g**) or even of the secondary aniline *N*-methylaniline (**2h**; 86–94% yield, Table 2, entries 8, 9, and 10) and low activated diphenylamine (**2i**; 73% yield, Table 2, entry 11). Interestingly, and despite the presence of a pyridyl substituent, which could potentially coordinate to the bimetallic intermediates involved in this process and inhibit their catalytic activity, the reaction of 3-aminopyridine (**2j**) with DIC gave guanidine **4l** in an 88% yield (Table 2, entry 12). This versatility and functional-group tolerance are remarkable when compared with other s-block

Table 2. Guanylation and hydrophosphination of carbodiimides.[a]

Entry	Amine/phosphine	Carbodiimide	Compound/Yield [%][b]
1	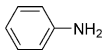	*i*PrN=C=N*i*Pr	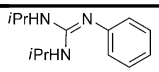
	2a	**3a**	**4a** (96)
2		CyN=C=NCy	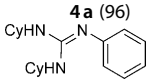
		3b	**4b** (90)
3		EtN=C=N*t*Bu	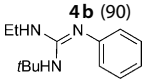
		3c	**4c** (80)
4	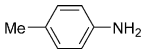	*i*PrN=C=N*i*Pr	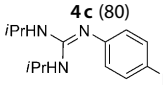
	2b	**3a**	**4d** (90)
5	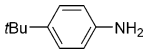	*i*PrN=C=N*i*Pr	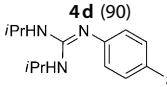
	2c	**3a**	**4e** (80)
6	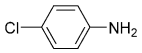	*i*PrN=C=N*i*Pr	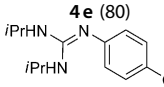
	2d	**3a**	**4f** (98)
7	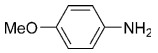	*i*PrN=C=N*i*Pr	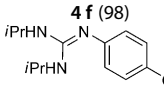
	2e	**3a**	**4g** (96)
8	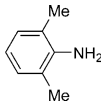	*i*PrN=C=N*i*Pr	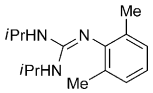
	2f	**3a**	**4h** (90)
9	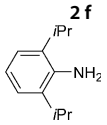	*i*PrN=C=N*i*Pr	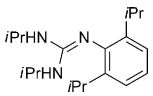
	2g	**3a**	**4i** (86)
10	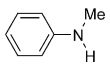	*i*PrN=C=N*i*Pr	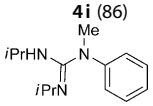
	2h	**3a**	**4j** (94)
11	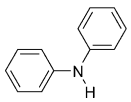	CyN=C=NCy	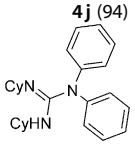
	2i	**3b**	**4k** (73)
12	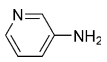	*i*PrN=C=N*i*Pr	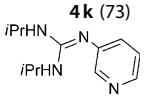
	2j	**3a**	**4l** (88)
13	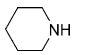	*i*PrN=C=N*i*Pr	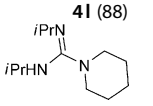
	2k	**3a**	**4m** (15); (52)[c]
14	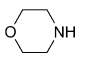	*i*PrN=C=N*i*Pr	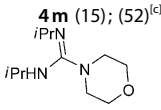
	2l	**3a**	**4n** (19); (65)[c]
15	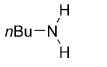	*i*PrN=C=N*i*Pr	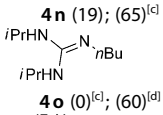
	2m	**3a**	**4o** (0)[c]; (60)[d]
16	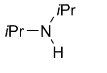	*i*PrN=C=N*i*Pr	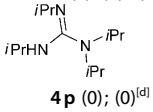
	2n	**3a**	**4p** (0); (0)[d]

Table 2. (Continued)

Entry	Amine/phosphine	Carbodiimide	Compound/Yield [%][b]
17	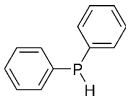	*i*PrN=C=N*i*Pr	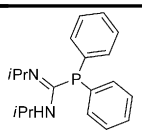
	2o	**3a**	**4q** (95)[e]
18		CyN=C=NCy	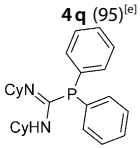
		3b	**4r** (90)[e]
19		EtN=C=N*t*Bu	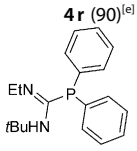
		3c	**4s** (80)

[a] Conditions: amine/phosphine (1.00 mmol), carbodiimide (1.00 mmol), catalyst **1** (2% mol), THF (3 mL), 1 h, 25 °C. [b] Isolated yields. [c] 1 h, 70 °C. [d] 24 h, 70 °C. [e] 30 min, 25 °C.

catalytic systems in which anilines with large substituents or coordinating groups give lower yields than nonsubstituted substrates.[9c,15] Cyclic amines morpholine and piperidine, and *n*-butylamine required the use of forcing reaction conditions, higher temperatures (70 °C), or a longer reaction time (24 h) to give guanidines **4m–o** in moderate yields (52–65%, Table 2, entries 13–15). In contrast, no reaction was observed when diisopropylamine (**2n**) was used, which can be rationalized in terms of the significant increase in steric bulk in this amine and its relatively low acidity compared with the other substrates studied (Table 2, entry 16). Although previous studies have shown the feasibility of homometallic magnesium complexes to catalyze guanylation processes by using unhindered amines,[16a,b] **1** offers a significant improvement for secondary amines and substituted anilines,[16a,c] and enables these processes to take place at room temperature over short periods of time. Interestingly, the hydrophosphination of carbodiimides **3a–c** with diphenylphosphine (**2o**) could also be achieved at room temperature by using catalyst loadings as low as 2 mol%, which afforded phosphoguanidines **4q–s** in high yields (80–95%, Table 2, entries 17–19). To the best of our knowledge, this represents the first example of a magnesium complex catalyzing this process, and shows an activity comparable to results with heavier alkaline-earth-metal amides reported by Hill et al., in which efficiency of the catalyst correlates directly with the increase in size of the metal cation.[18]

Stoichiometric studies

To gain mechanistic insights into these promising catalytic processes, a series of stoichiometric reactions were carried out. Addition of three molar equivalents of NH_2Ar (Ar = 2,6-$Me_2C_6H_3$; **2f**) to tris(alkyl)magnesiate **1** afforded colorless crys-

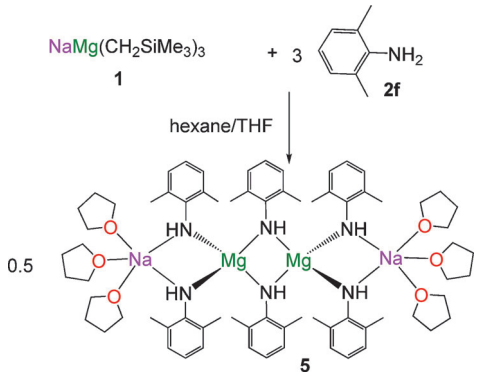

Scheme 3. Synthesis of sodium magnesiate **5**.

tals of tris(amido)magnesiate [{(THF)$_3$NaMg(NHAr$_3$)}$_2$] (**5**) in 58% yield (Scheme 3).

The molecular structure of **5** was determined by using X-ray crystallography, and was found to be dimeric and comprised of a tetranuclear Na···Mg···Mg···Na chain arrangement connected by six anilide bridges (see Figure 1).[21] This gives rise to three planar four-membered rings composed of two outer {NaN$_2$Mg} heterometallic rings linked through a central {Mg$_2$N$_2$} homometallic ring that is orthogonal to the outer rings. Each Mg atom in **5** is bonded to four amido groups with Mg–N contacts (mean value 2.08(5) Å) that are similar to those found in other reported tris(amido) alkali-metal magnesiates.[21] Three molecules of THF complete the coordination sphere of each sodium atom, which is also coordinated by two amido groups with Na–N contacts (mean value 2.54(4) Å) that are significantly elongated compared with that reported for the homometallic sodium anilide [{(PMDETA)NaNHPh}$_2$] (mean value 2.42(3) Å).[22] The structure of **5** contrasts with that previously reported by us for [(THF)$_2$NaMg(NPh$_2$)$_3$] (**6**). Compound **6** results from a similar reaction of **1** with three equivalents of diphenylamine, and displays a monomeric arrangement in which the amido groups coordinate terminally to Mg through their N atoms; whereas the Na center has π interactions with two phenyl groups in addition to binding to two THF ligands.[6]

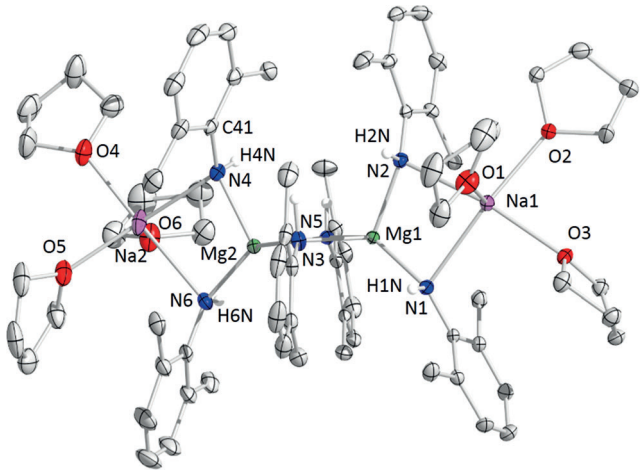

Figure 1. Molecular structure of [{(THF)$_3$NaMg(NAr$_3$)}$_2$] (**5**) with displacement ellipsoids drawn at the 30% probability level. Disorder and hydrogen atoms, except those attached to nitrogen atoms, are omitted for clarity. Selected bond lengths [Å] and angles [°]: Mg1–N1 2.032(2), Mg1–N2 2.051(2), Mg1–N3 2.159(2), Mg1–N5 2.111(2), Mg2–N3 2.078(2), Mg2–N4 2.057(2), Mg2–N5 2.160(2), Mg2–N6 2.028(2), Na1–N1 2.590(2), Na1–N2 2.539(2), Na1–O1 2.40(2), Na1–O 2.362(2), Na1–O3 2.356(2), Na2–N4 2.488(2), Na2–N6 2.562(2); N1-Mg1-N2 105.38(9), N1-Mg1-N3 106.75(9), N1-Mg1-N5 136.73(9), N2-Mg1-N3 102.89(8), N2-Mg1-N5 109.60(8), N3-Mg1-N5 89.58(7), N3-Mg2-N4 107.65(9), N3-Mg2-N5 90.45(8), N3-Mg2-N6 137.49(9), N4-Mg2-N5 101.10(9), N4-Mg2-N6 105.43(9), N5-Mg2-N6 108.59(8).

Multinuclear NMR spectroscopy characterization of compound **5** was performed in C_6D_6. ^{1}H NMR spectroscopy (Figure S5) revealed a complex spectrum with multiple signals in the aromatic, aliphatic, and NH regions. More informatively, the ^{13}C NMR spectrum showed six different signals (ranging from $\delta = 157.0$–152.7 ppm) that can be assigned to the *ipso*-C atoms of the 2,6-Me$_2$-C$_6$H$_4$ groups (Figure S6), which suggests a lack of equivalence between the anilide groups present in **5**. This is consistent with retention in C_6D_6 of the dimeric structure of **5** found in the solid state, with six nonequivalent anilide fragments derived from four chiral nitrogen atoms and two prochiral nitrogen atoms.[23] Further confirmation of the retention of the dimeric arrangement of **5** in C_6D_6 was gained by using ^{1}H DOSY NMR spectroscopy (see the Supporting Information). Investigation of a solution of **5** (40 mM) in deuterated toluene with tetramethylsilane (TMS) as an internal reference revealed *D* (diffusion coefficient) values of $5.076\,e^{-10}$ and $2.262\,e^{-09}$ m^2 s^{-1} (Figure S7 in the Supporting Information). By using the external calibration curve (ECC) for dissipated spheres and ellipsoids as elaborated by Stalke's group,[24] the molecular weight of compound **5** in solution was estimated to be 1183 g mol^{-1}. This result deviates by only 5% when compared to the dimeric structure observed for **5** in the solid state. Interestingly, in donor [D$_8$]THF as the solvent, DOSY experiments indicate the formation of solvent-separated ion-pair species (Scheme 4). In this case, two different diffusion coefficients were observed for **5** ($D_1 = 6.864\,e^{-10}$ and $D_2 = 5.929\,e^{-10}$ m^2 s^{-1}). From these values, two molecular weights were calculated ($M_{r1} = 773$ g mol^{-1} and $M_{r2} = 994$ g mol^{-1}),

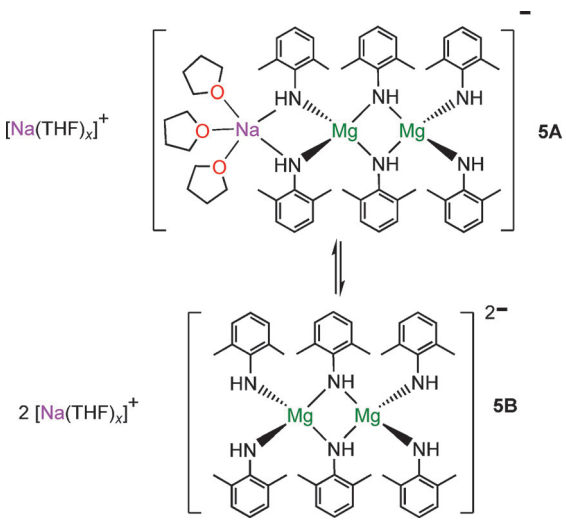

Scheme 4. Proposed magnesiate species **5A** and **5B** observed in [D$_8$]THF.

which are consistent with the presence in solution of monoanionic $[(THF)_3NaMg_2(NHAr)_6]^-$ (**5A**; (M_r = 769.66 g mol^{-1}) and dianionic $[Mg_2(NHAr)_6]^{2-}$ (**5B**; M_r = 1008.97 g mol^{-1}) species (1% error for both species).[25] Furthermore, 2D ^{1}H–^{1}H EXSY NMR data (Figures S10 and S11 in the Supporting Information) established that a slow exchange takes place between **5A** and **5B** in [D$_8$]THF.

^{1}H NMR spectroscopic monitoring of the reaction of an equimolar mixture of carbodiimide **3a** and aniline **2f** in the presence of 2 mol% of tris(amido) magnesiate **5** indicated the formation of guanidine **4h** in a 99% yield after 15 min at room temperature, which shows an identical efficiency to that found for tris(alkyl)magnesiate **1** (99%, Table 1, entry 3). This hints at a possible involvement of (amido)magnesiate **5** as an intermediate in the catalytic cycle (see above). If this is the case, the higher catalytic activity of **1** in the donor solvent THF compared with benzene (Table 1) can be rationalized in terms of the different constitutions of the relevant tris(amido) ate species in these solvents. THF favors the formation of solvent-separated ion-pair (SSIP) species that can be anticipated to be more powerful nucleophiles (with terminal Mg–N bonds) than the analogous contacted ion-pair (CIP) ates in which all the ligands are bridging between two metals.

We next investigated the insertion reactions of tris(amido) magnesiates **6** and **5** with three molar equivalents of carbodiimide **3b** and **3a**, respectively (Schemes 5 and 6, respectively). Interestingly, completely different outcomes were observed depending on the amido group present on the magnesiate. Compound **6**, with diphenylamido groups, can insert only two molecules of carbodiimide **3b** to give heteroleptic mixed amido/guanidinate sodium magnesiate **7** in 78% yield (Scheme 5). In

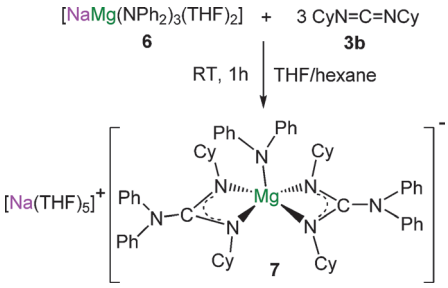

Scheme 5. Insertion reaction of **3b** with tris(amido) magnesiate **6**.

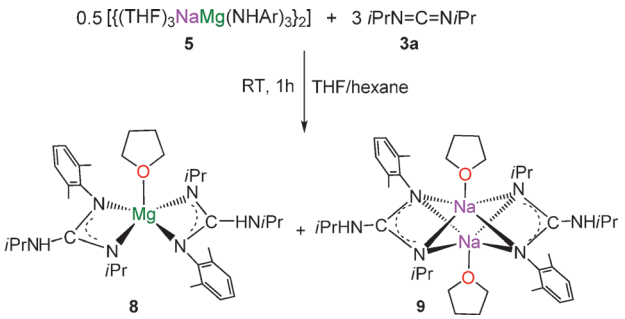

Scheme 6. Insertion reaction of **3a** with tris(amido) magnesiate **5**.

contrast, **5** can react effectively with three equivalents of **3a** to give a 1:1 mixture of homometallic magnesium and sodium guanidinates **8** and **9**, which contain the unsymmetrical guanidinate ligand [*i*PrNC(NH*i*Pr)NAr] that results from the formal insertion of the carbodiimide into the N–H bonds of the anilide groups present in **5** (Scheme 6).[26] The formation of [*i*PrNC(NH*i*Pr)NAr] can be rationalized as a result of a proton transfer from the arylamino nitrogen atom to an isopropylamido nitrogen followed by dissociation of the resultant NH*i*Pr group and formation of a new M–NAr bond (M = Mg or Na). This isomerization not only allows better stabilization of the negative charge of the ligand (due to the conjugation effect between the aromatic ring and the C=N bond), but also relief of the steric hindrance around the metal by replacing one bulky N*i*Pr arm of the guanidinate ligand with a NAr substituent.[27] Conversion of **5** into a 1:1 mixture of **8** and **9** occurs quantitatively, as indicated by ^{1}H NMR spectroscopic monitoring of the reaction. Compound **8** could be crystallized from the reaction mixture in 38% yield. Compound **9** could alternatively be prepared by insertion of **3b** in sodium amide $[\{(THF)_2Na(NHAr)\}_2]$ (**10**; see the experimental details in the Supporting Information).

These results suggest that under stoichiometric conditions, in the case of **5**, the insertion of a third equivalent carbodiimide into the remaining anilide group induces the disproportionation of putative magnesiate $[\{Na(THF)_x\}[Mg\{iPrNC(NHiPr)NAr\}_3]$ into its monometallic guanidinate components **8** and **9**. This process is probably driven by the high steric congestion around Mg when coordinated by three guanidinate ligands. Attempts to prepare the relevant products of insertion that result from the reactions of one and two equivalents of DIC with **5** gave, in all cases, variable amounts of **8** and **9** (in 1:1 ratio) along with the recovery of unreacted **5**. Thus, under the conditions of this study, it appears that the threefold activation of the Mg–NHAr bonds of **5** is significantly favored over a possible sequential reactivity. In contrast, sodium magnesiate **7** does not react with a further equivalent of carbodiimide even under forcing reaction conditions (12 h, 60 °C). This lack of reactivity can be attributed to the steric congestion around Mg in **7**, which should compromise not only the approach of the heterocumulene to the magnesiate anion but also the availability of the remaining NPh_2 amido group to act as a nucleophile, with its N atom sheltered by the cyclohexyl scaffolding of the guanidinate ligands (see Figure 2, right, for a space-filling model) and also further stabilized by delocalization of its lone pair across its two Ph substituents (sum of the angles around N7 = 359.9°; see Figure 2, left).

X-ray crystallographic studies established the molecular structures of **7**, **8**, and **9** (Figures 2–4, respectively). Sodium magnesiate **7** exhibits a SSIP structure comprised of a sodium cation solvated by THF molecules, balanced by a magnesiate anion in which the magnesium center is bound by two chelating guanidinate ligands and a terminal NPh_2 group (Figure 2, left). The five-coordinate Mg center displays a distorted square planar pyramidal geometry (total bond angles around base = 338°), in which the NPh_2 ligand occupies the apical position (Figure 2, left).

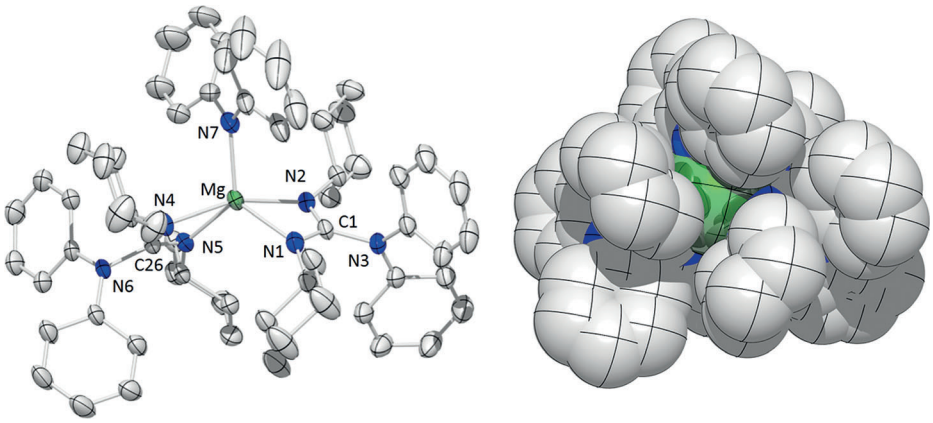

Figure 2. Left: Molecular structure of the $[Mg\{(CyN)_2C(NPh_2)\}_2(NPh_2)]^-$ anion present in **7** with displacement ellipsoids drawn at the 30% probability level. Hydrogen atoms are omitted for clarity. Right: Space-filling model for this anion. Selected bond lengths [Å] and angles [°]: Mg–N(1) 2.116(3), Mg–N2 2.194(3), Mg–N4 2.178(3), Mg–N5 2.130(3), N1–C1 1.326(5), N2–C1 1.299(5), N3–C1 1.440(5), N4–C26 1.304(5), N5–C26 1.309(5), N6–C26 1.469(4); N1-Mg-N7 120.16(15), N1-Mg-N2 62.4(1), N1-Mg-N5 114.8(1), N2-Mg-N4 160.9(1), N2-Mg-N7 100.0(1), N4-Mg-N5 62.5(1), N4-Mg-N7 99.0(1), N5-Mg-N7 125.1(1).

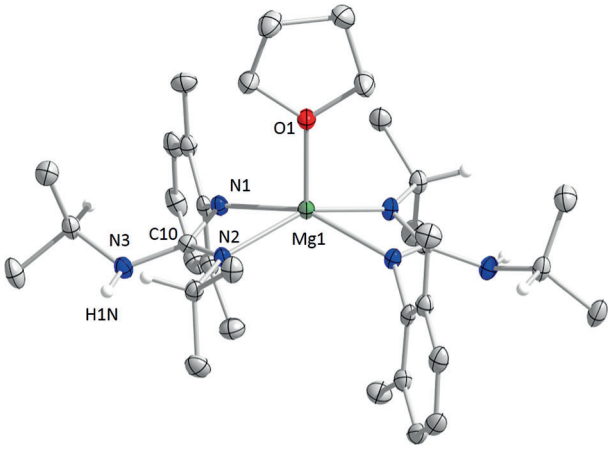

Figure 3. Molecular structure of $[Mg\{(i\text{PrNC(NAr)}\{(\text{HN}i\text{Pr})\}_2(\text{THF})]$ (**8**; Ar = 2,6-$Me_2C_6H_3$) with displacement ellipsoids drawn at the 30% probability level. Hydrogen atoms, except those attached to nitrogen atoms and those on the CH groups of the isopropyl substituents, are omitted for clarity. Selected bond lengths [Å] and angles [°]: Mg1–O1 2.039(2), Mg1–N1 2.158(2), Mg1–N2 2.066(2), N1–C10 1.344(3), N2–C10 1.326(3), N3–C10 1.385(3), N3–H1N 0.84(4); O1-Mg1-N1 163.65(6), O1-Mg1-N2 104.94(7), N1-Mg1-N2 64.01(8), N2-Mg1-N1′ 108.45(8).

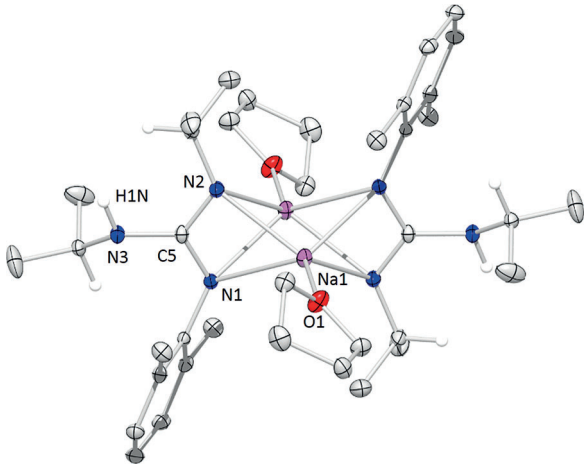

Figure 4. Molecular structure of $[Na\{(i\text{PrNC(NAr)}(\text{HN}i\text{Pr})\}(\text{THF})]_2$ (**9**; Ar = 2,6-$Me_2C_6H_3$) with displacement ellipsoids drawn at the 30% probability level. Hydrogens atoms, except those attached to nitrogen atoms and those on the CH groups of the isopropyl substituents, are omitted for clarity. Selected bond lengths [Å] and angles °]: Na1–O1 2.277(1), Na1–N1 2.453(1), Na1–N2 2.558(2), N1–C5 1.341(2), N2–C5 1.323(2), N3–C5 1.404(2), N3–H1N 0.9(2); O1-Na1-N1 122.19(4), O1-Na1-N2 123.79(4), O1-Na1-N1′ 122.27(5), O1-Na1-N2′ 120.48(4), N1-Na1-N2 53.57(4), N2-Na1-N1′ 89.20(5), N2′-Na1-N1 93.88(5), N1-C5-N2 116.0(1), N1-C5-N3 120.4(1), N2-C5-N3 123.5(1).

Although, as far as we are aware, **7** constitutes the first example of an alkali-metal magnesiate with guanidinate ligands to be structurally defined, the structure of the magnesiate anion bears a strong resemblance to that found for homometallic magnesium complex **8** (Figure 3), though in this case the apical position is filled by a molecule of the neutral donor THF. Structures related to that of **8** have recently been reported by Kays et al. for magnesium guanidinates, obtained by using an alternative synthetic approach of $Mg\textit{n}Bu_2$ deprotonation of guanidines with highly sterically demanding groups.[28,29] It should also be noted that the guanidinate ligands present in **8** are unsymmetrical, with one of the chelating N′ atoms attached to *i*Pr (N1), whereas the remaining N atom (N2) binds to 2,6-dimethylphenyl (Ar; see above). This lack of symmetry translates to the formation of noticeably shorter Mg–NR bonds if R = *i*Pr (2.066(2) Å) than for the aromatic substituent (2.158(2) Å).

Sodium guanidinate **9** shows a dimeric arrangement with the two guanidinate ligands parallel to each other (Figure 4). Each sodium is coordinated by four N atoms of the Na_2N_4 core (contacts range from 2.453(1) to 2.558(2) Å) and a molecule of THF, with a Na···Na1 vector of length 2.671(2) Å, which lies perpendicular to the two guanidinate NCN planes. Although it contains the same unsymmetrical guanidinate ligand described above for **8**, an opposite trend is observed for the length of the Na–N bonds (Na–N1 2.453(1) Å vs. Na–N2, 2.558(2) Å) in **9**. The structure of **9** contrasts with that reported for trimeric

guanidinate complex $\{Na[CyNC(N(SiMe_3)_2)NCy]\}_3$, which results from the reaction of DCC with $NaN(SiMe_3)_2$.[30]

Protonolysis of guanidinate complexes **7**–**9** was attempted by treating them with variable amounts of the relevant amine (two equivalents of $NHPh_2$ for **7**, and two and one equivalents of NH_2Ar for **8** and **9**, respectively). In all cases, no reaction was apparent after 24 h at room temperature. The catalytic ability of these guanidinate complexes was also investigated. Interestingly, mixed-metal guanidinate **7** was able to catalyze the guanylation of DCC with $NHPh_2$ to give guanidine in almost identical yields to those found by using sodium magnesiate **1** (73% vs. 75%; conditions in both cases: 2 mol% catalyst loading, RT, 1 h). However, illustrating the synergistic capabilities in sodium magnesiate systems, single-metal guanidinates **8** and **9** displayed significantly lower efficiencies for the reaction of DIC and NH_2Ar than **1**. Thus Mg complex **8** afforded the guanidine product in a modest 30% yield after 15 min, whereas Na complex **9** gave 72% conversion under the same conditions. Even when an equimolar mixture of **8** and **9** was employed as a catalyst for this reaction (2 mol% loading, RT, 15 min), the observed conversions were still lower (76%) than when using preformed bimetallic precatalyst **1** (99%). Collectively, despite the isolation of single-metal complexes in some of the stoichiometric studies, these results support the view that these guanylation reactions are indeed ate-catalyzed transformations and highlight the limitations of comparing the results of stoichiometric reactions with the complex equilibria present during catalytic processes in which variable excesses of reagents are present.

Mechanistic studies

The observations from our stoichiometric studies, together with knowledge obtained from previous reports on s-block single-metal catalysts,[9] suggest that these ate-catalyzed guanylation reactions of amines may take place by the mechanism presented in Scheme 7. Initially, fast protonation of sodium tris(alkyl) magnesiate **1** takes place to form a nucleophilic sodium tris(amido) magnesiate (as seen for **5** and **6**), which in turn can undergo carbodiimide insertion to give a sodium magnesiate guanidinate complex. Protonolysis of this latter species with one equivalent of amine liberates the guanidine product and regenerates the active sodium tris(amido) magnesiate.

Previous insightful mechanistic studies by Richeson et al. with LiHMDS as a catalyst have shown that the insertion step in these processes is initiated by coordination of the carbodiimide to the Lewis acidic Li center.[31] By using bimetallic **1** as a precatalyst, two potential sites are available for coordination through either the Na or Mg centers. Repeating the guanylation of DIC (**3a**) by 2,6-dimethylaniline (**2f**) with a 1:1 mixture of sodium magnesiate **1** and the crown ether 15-crown-5 (which can block Na coordination sites) as a catalyst showed only a slight decrease in the yield of guanidine **4h** (from 99 to 83%). Coupled with the DOSY studies that show preference of these bimetallic compounds to exist as SSIP structures in THF, this suggests only a secondary role for sodium in this process, with pre-coordination of the carbodiimide to Mg. Consistent with this interpretation of a minor involvement of the alkali metal, rather than stabilizing the magnesiate anion, using the lithium derivative $[LiMg(CH_2SiMe_3)_3]$[32] as a precatalyst led to conversions (97%) that were almost identical to those observed when using sodium-containing **1**. Thus, the enhanced catalytic activity of these bimetallic systems seems to be a case of anionic activation,[33] in which the formation of magnesiate anions generates more powerful nucleophilic intermediates than by using charge-neutral organomagnesium precursors.[16]

To obtain quantitative kinetic data, reactions of *N*,*N*′-diisopropylcarbodiimide with 4-*tert*-butylaniline in the presence of **1** as the catalyst were carried out in $[D_8]$THF as the solvent. Reaction rates of the guanylation were monitored over time by using ^1H NMR spectroscopy and using the integration changes in the substrate resonances over more than three half-lives. We first determined the order of the reaction with respect to amine concentration by keeping the concentration of other components virtually unaltered. The study was started by using 2 mol% of catalyst **1** and the carbodiimide/amine molar ratio was kept at 10:1 to maintain approximately zero-order conditions for carbodiimide. The plot of $\ln([A]_0/[A]_t)$ versus reaction time is shown in Figure 5, in which $[A]_0$ is the initial amine concentration and $[A]_t$ is the amine concentration after a given reaction time. An induction period was not observed, which indicates that the catalyst was reactive from the begin-

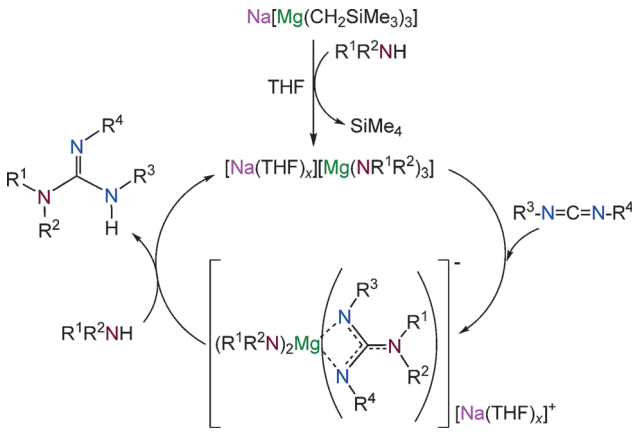

Scheme 7. Proposed mechanism for the guanylation of anilines with **1**.

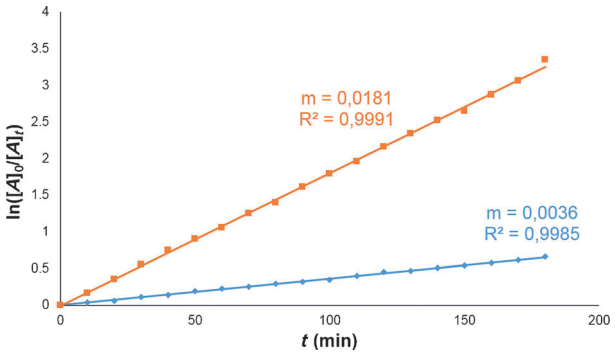

Figure 5. First-order kinetic analysis of the NMR-tube scale reaction of 4-*tert*-butylaniline (■) or 4-*tert*-butylaniline-$[D_2]$ (◆) and diisopropylcarbodiimide in $[D_8]$THF with 2 mol% of **1** at RT.

ning of the process. The data confirm a fit consistent with first-order kinetic behavior with respect to amine concentration.

Next, we determined the order of the reaction with respect to the concentration of carbodiimide. During this study, we maintained a relative carbodiimide/amine ratio of 1:10, and the linearity of the plot of $\ln([C]_0/[C]_t)$, in which [C] is the carbodiimide concentration, versus reaction time shows that the reaction was also first order with respect to this reagent (Figure S22 in the Supporting Information). Additionally, we carried out a H/D kinetic isotope effect (KIE) experiment by using *N*,*N*′-diisopropylcarbodiimide and [D_2]-4-*tert*-butylaniline with catalyst **1**. This study gave a KIE (k_H/k_D) value of 5 (Figure 5). The maximum calculated kinetic isotope effect (KIE) at 25 °C for a reaction that involves a N–H bond should be approximately 8.5. In the guanylation reaction of *tert*-butylaniline, the magnitude of the measured value was clearly indicative of a primary KIE[34] and indicates that a N–H bond is broken during the turnover-limiting step. Although this observation would indicate that protonolysis of the starting alkyl compound by the amine could be the rate-determining step, it seems unlikely because stoichiometric reactions demonstrate that these protolytic reactions occur instantaneously at room temperature. Thus, the more limiting protonolysis of chelate guanidinate intermediates could be responsible for this high KIE.

The dependence of the rate of reaction with respect to catalyst concentration was studied at different catalyst precursor concentrations ([**1**] = 1–5 mol%) with the carbodiimide/amine molar ratio fixed at 10:1. A plot of reaction rate versus catalyst concentration reveals a linear increase in the reaction rate with catalyst concentration (Figure 6, left).

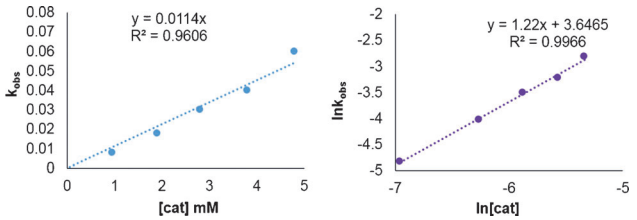

Figure 6. Plot of reaction rate versus concentration of the catalyst (left) and van 't Hoff plot (right).

The first-order rate of the reaction with respect to catalyst concentration was further confirmed from the van 't Hoff plot for the three first concentrations (Figure 6 right). The value of the slope was determined to be close to 1. Thus, from the present study, the overall rate law for the guanylation of 4-*tert*-butylaniline with *N*,*N*′-diisopropylcarbodiimide catalyzed by **1** at low concentrations could be summarized as shown in Equation (1). A similar rate law has been obtained for trinuclear zirconium alkyl diamido complexes.[34]

$$\text{rate} = k[\text{amine}]^1[\text{carbodiimide}]^1[\text{catalyst}]^1 \quad (1)$$

Values of k_{obs} at four different temperatures were measured. These k_{obs} values satisfactorily fit the Arrhenius plot (Figure 7,

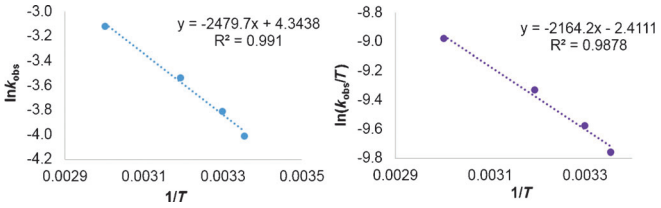

Figure 7. Arrhenius (left) and Eyring plots (right) for the guanylation reaction catalyzed by **1**.

left) with an E_a value of 20.7 kJ mol^{-1}. The activation parameters were quantified by a plot of $\ln(k_{obs}/T)$ versus $1/T$, which results in $\Delta H^{\neq} = 18.1$ kJ mol^{-1} and $\Delta S^{\neq} = -25.8$ J mol^{-1} K^{-1} (Figure 7, right).[35] This last value could support the existence of a concerted transition state. Although the kinetic studies of the guanylation process are scarce,[16a,35] several authors have proposed an amine-assisted concerted transition state in comparatively analogous alkene hydroamination processes with Group 2 metal complexes that involve, as in this case, a large isotopic effect.[2a,36] This amine-assisted state could also explain the first order observed with respect to amine (and carbodiimide). Under catalytic conditions, in which an excess of amine is present through the main part of the process, we propose that the magnesium amido complex formed in the first step could coordinate an amine molecule so that the negatively charged nitrogen atom of the incoming carbodiimide is stabilized, which favors the attack of an amido ligand on the electrophilic carbon atom (Figure 8).

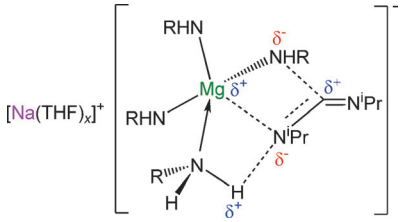

Figure 8. Proposed carbodiimide insertion transition state.

Conclusion

We report herein the first catalytic applications of alkali-metal magnesiates for guanylation and hydrophosphination reactions. A homoleptic mixed Na/Mg complex, [$NaMg(CH_2SiMe_3)_3$] (**1**), has been found to offer significantly greater catalytic ability than that of its homometallic components [$NaCH_2SiMe_3$] and [$Mg(CH_2SiMe_3)_2$], which allows guanylation of a range of substituted anilines and secondary amines under very mild reaction conditions (in most cases, at RT). Furthermore, by installing Mg within this sodium magnesiate platform, it is possible to activate it towards catalysis of the hydrophosphination of carbodiimides at room temperature.

Stoichiometric investigations have allowed the isolation and structural elucidation of tris(amido) sodium magnesiate [{$(THF)_3NaMg(NHAr_3)$}$_2$] (**5**) and mixed amido/guanidinate

sodium magnesiate $[Na(THF)_5]^+[Mg\{(CyN)_2C(NPh_2)\}_2(NPh_2)]^-$ (**7**). These appear to be intermediates in these catalytic transformations. Reactivity studies in these complexes, coupled with kinetic investigations, suggest these guanylation reactions occur by forming highly nucleophilic (tris)amide intermediates that can subsequently react with the carbodiimide in an insertion step, followed by amine protonolysis of the resultant guanidinate species. Interestingly, all these processes appear to take place in the coordination sphere of Mg, with Na taking a backseat in the catalytic cycle and stabilizing the magnesiate anion intermediates, which hints that the enhanced catalytic activity of these systems is due to anionic activation.

The rate law for the guanylation of *N*,*N*′-diisopropylcarbodiimide with 4-*tert*-butylaniline catalyzed by **1** was deduced to be first order with respect to [amine], [carbodiimide], and [catalyst] and shows a large kinetic isotopic effect, which is consistent with the formation of an amine-assisted rate-determining carbodiimide insertion transition state.

Experimental Section

General considerations

All reactions were performed under a protective argon atmosphere by using standard Schlenk techniques. Hexane, benzene, and THF were dried by heating to reflux over sodium benzophenone ketyl and distilled under nitrogen or were passed through a column of activated alumina (Innovative Tech.), degassed under nitrogen, and stored over molecular sieves in the glovebox prior to use. $Mg(CH_2SiMe_3)_2$, $NaCH_2SiMe_3$, $[NaMg(CH_2SiMe_3)_3]$, and $[(THF)_2NaMg(NPh_2)_3]$ were prepared according to literature procedures.[6,19,37] $LiCH_2SiMe_3$, amines, phosphines, and carbodiimides were purchased from Sigma–Aldrich and used as received. NMR spectra were recorded by using a Bruker DPX400 MHz spectrometer operated at 400.13 (^{1}H) or 100.62 MHz (^{13}C), or by using a Varian FT-400 spectrometer with standard VARIAN-FT software. Elemental analyses were carried out by using a Perkin–Elmer 2400 elemental analyzer.

Preparative scale reaction of the guanidines and phosphaguanidines

In a glovebox, a solution of compound **1** (2% mol) in THF (3 mL) was added in a Schlenk tube. Amine (or phosphane; 1.00 mmol) and carbodiimide (1.00 mmol) were then added to the above reaction mixture. The Schlenk tube was removed from the glovebox and the reaction was stirred at the desired temperature. After carrying out the reaction for the desired time, the solution was concentrated under reduced pressure, hexane was added, and the mixture was placed in a refrigerator at −30 °C for 16 h. After filtration, the products were obtained as white microcrystalline solids and characterized by comparing their NMR spectra with the literature data.[14a,e,16a,27,38]

X-ray crystallography

Data for samples **5**, **8**, and **9** were measured by using Oxford Diffraction diffractometers[39] with $Mo_{K\alpha}$ ($\lambda = 0.71073$ Å) or $Cu_{K\alpha}$ ($\lambda = 1.5418$ Å). Data for sample **7** were measured at Beamline I19 of the Diamond Light Source with $\lambda = 0.6889$ Å radiation and a Crystal Logics diffractometer with Rigaku Saturn 724+ CCD detector; data collection and processing was performed by using Rigaku and Bruker software. All structures were refined to convergence on F^2 of all independent reflections by using the full-matrix least-squares method in the SHELXL program.[40] Selected crystallographic and refinement details are given in Table S1 in the Supporting Information.

$[\{(THF)_3NaMg(NHAr)_3\}_2]$ (5; Ar = 2,6-$Me_2C_6H_3$)

2,6-Dimethylaniline (3 mmol, 0.37 mL) was added to a suspension of $NaMg(CH_2SiMe_3)_3$ (1 mmol, 0.309 g) in hexane (10 mL). After stirring for 1 h at RT, THF (2 mL) was added to give a light-brown solution. The solution was stored at −20 °C overnight to give colorless crystals of sodium magnesiate **5** (0.362 g, 58%). ^{1}H NMR (400 MHz, 298 K, C_6D_6): $\delta = 1.24$ (m, 24H; THF), 1.87, 1.98, 2.07, 2.18, 2.19, 2.22 (36H; C*H*$_3$, NH*Ar*), 2.52, 2.57, 2.68, 2.76, 2.79, 2.81 (6H; NH*Ar*), 3.19 (m, 24H; THF), 6.3–7.1 ppm (18H; C*H*, NH*Ar*); ^{13}C NMR (100 MHz, 298 K, C_6D_6): $\delta = 18.8$, 19.5, 19.7, 20.0, 20.9, 21.6 (*C*H$_3$, NH*Ar*), 25.5 (THF), 67.8 (THF), 111.7, 111.8, 112.3, 112.6, 116.6, 121.4, 121.7, 122.0, 124.7, 125.3, 125.9, 128.6, 128.9, 129.0, 129.1, 129.3, 129.5, 129.8 (*C*H, NH*Ar*), 152.7, 152.8, 156.1, 156.2, 156.6,157 ppm (*ipso-C*, NH*Ar*); elemental analysis calcd (%) for $C_{72}H_{108}Mg_2N_6Na_2O_6$: C 69.28, H 8.72, N 6.73; found: C 69.25, H 8.85, N 7.12.

$[Na(THF)_5]^+[Mg\{(CyN)_2C(NPh_2)\}_2(NPh_2)]^-$ (7)

N,*N*′-Dicyclohexylcarbodiimide (DCC (**3a**); 0.62 g, 3 mmol) was added to a solution of sodium magnesiate $[(THF)_2NaMg(NPh_2)_3]$ (**6**; 0.7 g, 1 mmol) in THF (4 mL). After stirring for 1 h, hexane (4 mL) was added and the Schlenk tube was stored in the freezer (−30 °C) overnight to allow the formation of colorless crystals of $[Na(THF)_5]^+[Mg\{(CyN)_2C(NPh_2)\}_2(NPh_2)]^-$ (**7**; 1.03 g, 78%). ^{1}H NMR (400 MHz, 298 K, C_6D_6): $\delta = 1.04$–1.27, 1.47–1.73 (m, 40H; C*H*$_2$, CyN), 1.43 (m, 20H; THF), −3.40–4.48 (m, 4H; C*H*, CyN), 3.57 (m, 20H; THF), 6.71 (t, $J = 7.1$ Hz, 1H; N*Ph*$_2$), 6.79 (t, $J = 7.1$ Hz, 1H; N*Ph*$_2$), 6.85–6.90 (m, 4H; C*H*, N*Ph*$_2$, guanidinate), 7.16–7.23, (m, 8H; C*H*, N*Ph*$_2$, guanidinate), 7.28–7.38 (m, 4H; C*H*, N*Ph*$_2$), 7.44 (d, $J = 7.6$ Hz, 8H; N*Ph*$_2$, guanidinate), 7.50 (d, $J = 7.6$ Hz, 2H; N*Ph*$_2$), 7.67 ppm (d, $J = 7.6$ Hz, 2H; N*Ph*$_2$); ^{13}C NMR (100 MHz, 298 K, C_6D_6): $\delta = 25.7$ (THF), 26.2, 26.5, 26.6, 26.8, 37.3, 37.4, (*C*H$_2$, CyN) 55, 56.1 (*C*H, CyN), 67.9 (THF), 121.1, 129.3, 130.2 (*C*H, N*Ph*$_2$, guanidinate), 145.8 (*ipso-C*, N*Ph*$_2$, guanidinate), 122, 129.5, 130.3 (*C*H, N*Ph*$_2$), 146.3 (*ipso-C*, N*Ph*$_2$), 163.5 ppm (*C*N$_3$); elemental analysis calcd (%) for $C_{82}H_{114}MgN_7NaO_5$: C 74.32, H 8.67, N 7.40; found: C 74.48, H 8.41, N 8.37.

Stoichiometric studies: reaction between 5 and 3a

Sodium magnesiate $[\{(THF)_3NaMg(NHAr_3)\}_2]$ (**5**; 0.312 g, 0.25 mmol) was reacted with *N*,*N*′-diisopropylcarbodiimide (1.5 mmol, 0.23 mL) in THF (2 mL). The reaction mixture was stirred for 1 h, then hexane (4 mL) was added (if a precipitate formed, it was redissolved with gentle heating). The solution was stored at −15 °C overnight to allow the formation of colorless crystals of $[Mg\{(iPrN)C(NAr)(HNiPr)\}_2(THF)]$ (**8**; 112 mg, 38%). ^{1}H NMR (400 MHz, 298 K, $[D_8]$THF): $\delta = 0.56$ (d, $J = 6.2$ Hz, 12H; C*H*$_3$, *i*Pr), 0.79 (d, $J = 6.4$ Hz, 12H; C*H*$_3$, *i*Pr), 1.77 (m, 4H; THF), 2.19 (s, 12H; C*H*$_3$, N*Ar*), 3.02–3.15 (m, 4H; C*H*, *i*Pr), 3.61 (m, 4H; THF) 3.80 (br d, 2H; NH*i*Pr), 6.56 (t, $J = 7.6$ Hz, 2H; *para*-C*H*, N*Ar*), 6.80 ppm (d, $J = 7.6$ Hz, 4H; *meta*-C*H*, N*Ar*); ^{13}C NMR (100 MHz, 298 K, $[D_8]$THF): $\delta = 19.7$ (*C*H$_3$, N*Ar*), 24.2 (*C*H$_3$, *i*Pr), 25 (*C*H$_3$, *i*Pr), 26.2 (THF), 44.7 (*C*H, *i*Pr), 45.0 (*C*H, *i*Pr), 68.0 (THF), 120.1 (*para*-*C*H, N*Ar*), 128.1 (*meta*-*C*H, N*Ar*), 132.6 (*ortho-C*, N*Ar*), 150.3 (*ipso-C*, N*Ar*), 163.5 ppm (*C*N$_3$); elemental analysis calcd (%) for $C_{34}H_{56}MgN_6O$: C 69.31, H 9.58, N 14.26; found: C 68.73, H 9.26, N 13.97.

[Na{(*i*PrN)C(NAr)(HN*i*Pr)}(THF)]$_2$ (9; Ar = 2,6-Me$_2$C$_6$H$_3$)

N,*N*′-Diisopropylcarbodiimide (0.08 mL, 0.5 mmol) was added to a solution of sodium (2,6-dimethylphenyl)amide [{Na(NHAr)}$_2$] (**10**; 0.143 g, 0.5 mmol) in hexane/THF (5 mL, 4:1 v/v). The resulting pale-yellow solution was stored in the freezer (−30 °C) overnight to allow the formation of colorless crystals of [Na{(*i*PrN)C(NAr)(HN*i*Pr)}(THF)]$_2$ (**9**; 0.108 g, 63%). ^{1}H NMR (400 MHz, 298 K, [D$_8$]THF): δ = 0.91 (s, 24H; C*H*$_3$, *i*Pr), 1.78 (m, 4H; THF), 2.11 (s, 6H; C*H*$_3$, N*Ar*), 3.30 (br s, 4H + 2H; C*H*, *i*Pr + N*H*i*Pr*), 3.61 (m, 4H; THF), 6.26 (t, *J* = 7.2 Hz, 2H; *para*-C*H*, N*Ar*), 6.69 ppm (d, *J* = 7.2 Hz, 4H; *meta*-C*H*, N*Ar*).; ^{13}C NMR (100 MHz, 298 K, [D$_8$]THF): δ = 19.8 (*C*H$_3$, N*Ar*), 24.4 (*C*H$_3$, *i*Pr), 26.2 (THF), 27.0 (*C*H$_3$, *i*Pr), 44.6 (*C*H, *i*Pr), 46.7 (*C*H, *i*Pr), 115.3 (*ortho*-C, N*Ar*), 127.7 (*meta*-*C*H, N*Ar*), 129.7 (*para*-*C*H, N*Ar*), 155.3 (*ipso*-C, N*Ar*), 160.2 ppm (*C*N$_3$); elemental analysis calcd (%) for C$_{34}$H$_{56}$N$_6$Na$_2$O (one molecule of THF per dimer was considered, based on the NMR data): C68.50, H 9.24, N 13.76; found: C 67.14, H 9.22, N 14.51.

General procedure for kinetic experiments

Kinetic experiments were performed by using a Varian FT-400 MHz spectrometer, and a standard solution of catalyst **1** in deuterated THF was used. The described kinetic experiments were carried out on *N*,*N*′-diisopropylcarbodiimide **3a** and 4-*tert*-butilaniline **2c** to form the corresponding guanidine. Reactions were carried out in J-Young NMR tubes and the reaction rates were measured by monitoring the disappearance of amine (or carbodiimide) and the formation of guanidine by using ^{1}H NMR spectroscopy at the described intervals over more than three half-lives. All data were processed by using Varian integral analysis software. Reaction rates were derived from the plot of Ln[substrate]$_0$/[substrate] vs. time (by fitting data to the equation Ln[substrate]$_0$/[substrate] = $k_{obs}t$) by using linear trend lines generated by using Microsoft Excel software. To obtain Arrhenius and Eyring plots, kinetic analyses were conducted at four different temperatures, each separated by approximately 5–10 K.

Determination of reaction order with respect to aniline 2c and carbodiimide 3a

The order of the reaction with respect to amine concentration was determined by keeping the concentration of the other components virtually unaltered, using a 1.9 mM solution of catalyst **1**, and using a carbodiimide/amine molar ratio greater than 10:1. The excess carbodiimide concentration maintains approximately zero-order conditions. The order of the reaction with respect to the concentration of carbodiimide was studied at an amine/carbodiimide molar ratio higher than 10:1.

Acknowledgements

We thank the University of Strathclyde (studentship to Z.L.) and the European Research Council (ERC-STG grant to E.H.) for generous sponsorship of this research, and the Spanish Ministerio de Economía y Competitividad (MINECO) for support under project CTQ2014-51912-REDC. We also thank Diamond Light Source for access to beamline I19. A.M., F.C.-H., and A. A. gratefully acknowledge financial support from the Junta de Comunidades de Castilla-La Mancha (project PEII-2014-041-P).

Keywords: cooperative effects · guanidines · homogeneous catalysis · magnesiates · s-block metals

[1] For reviews on Group 2 catalysis, see: a) M. S. Hill, D. J. Liptrot, C. Weetman, *Chem. Soc. Rev.* **2016**, *45*, 972; b) S. Harder, *Chem. Rev.* **2010**, *110*, 3852; c) A. G. M. Barrett, M. R. Crimmin, M. S. Hill, P. A. Procopiou, *Proc. R. Soc. London Ser. A* **2010**, *466*, 927.

[2] a) C. Brinkmann, A. G. M. Barrett, M. S. Hill, P. A. Procopiou, *J. Am. Chem. Soc.* **2012**, *134*, 2193; b) C. Weetman, M. D. Anker, M. Arrowsmith, M. S. Hill, G. Kociok-Kohn, D. J. Liptrot, M. F. Mahon, *Chem. Sci.* **2016**, *7*, 628; c) D. J. Liptrot, M. S. Hill, M. F. Mahon, A. S. S. Wilson, *Angew. Chem. Int. Ed.* **2015**, *54*, 13362; *Angew. Chem.* **2015**, *127*, 13560; d) M. D. Anker, M. S. Hill, J. P. Lowe, M. F. Mahon, *Angew. Chem. Int. Ed.* **2015**, *54*, 10009.

[3] a) J. Penafield, L. Maron, S. Harder, *Angew. Chem. Int. Ed.* **2015**, *54*, 201; *Angew. Chem.* **2015**, *127*, 203; b) J. Intemann, H. Bauer, J. Pahl, L. Maron, S. Harder, *Chem. Eur. J.* **2015**, *21*, 11452; c) J. Intemann, M. Lutz, S. Harder, *Organometallics* **2014**, *33*, 5722.

[4] B. Liu, T. Roisnel, J. F. Carpentier, Y. Sarazin, *Angew. Chem. Int. Ed.* **2012**, *51*, 4943; *Angew. Chem.* **2012**, *124*, 5027.

[5] a) J.-S. Ryu, G. Y. Li, T. J. Marks, *J. Am. Chem. Soc.* **2003**, *125*, 12584; b) D. V. Gribkov, K. C. Hultzsch, F. Hampel, *J. Am. Chem. Soc.* **2006**, *128*, 3748.

[6] A. Hernán-Gómez, T. D. Bradley, A. R. Kennedy, Z. Livingstone, S. D. Robertson, E. Hevia, *Chem. Commun.* **2013**, *49*, 8659.

[7] a) T. Klatt, J. T. Markiewicz, C. Saemann, P. Knochel, *J. Org. Chem.* **2014**, *79*, 4253; b) A. Harrison-Marchand, F. Mongin, *Chem. Rev.* **2013**, *113*, 7470; c) F. Mongin, A. Harrison-Marchand, *Chem. Rev.* **2013**, *113*, 7563; d) R. E. Mulvey, S. D. Robertson, *Top Organomet Chem* **2014**, *45*, 103.

[8] For selected references on alkali-metal magnesiates, see: a) N. Boudet, J. R. Lachs, P. Knochel, *Org. Lett.* **2007**, *9*, 5525; b) L. Shi, Y. Chu, P. Knochel, H. Mayr, *Angew. Chem. Int. Ed.* **2008**, *47*, 202; *Angew. Chem.* **2008**, *120*, 208; c) A. Krasovskiy, V. Krasovskaya, P. Knochel, *Angew. Chem. Int. Ed.* **2006**, *45*, 2958; *Angew. Chem.* **2006**, *118*, 3024; d) S. H. Wunderlich, C. J. Rohbogner, A. Unsinn, P. Knochel, *Org. Process Res. Dev.* **2010**, *14*, 339; e) D. Tilly, F. Chevallier, F. Mongin, P. C. Gros, *Chem. Rev.* **2014**, *114*, 1207; f) C. Y. Liu, P. Knochel, *Org. Lett.* **2005**, *7*, 2543; g) R. J. Kloetzing, A. Krasovskiy, P. Knochel, *Chem. Eur. J.* **2006**, *12*, 215; h) F. F. Fleming, V. Gudipati, O. W. Steward, *Org. Lett.* **2002**, *4*, 659; i) J. Kondo, A. Inoue, H. Shinokubo, K. Oshima, *Angew. Chem. Int. Ed.* **2001**, *40*, 2085; *Angew. Chem.* **2001**, *113*, 2146; j) P. C. Andrikopoulos, D. R. Armstrong, D. V. Graham, E. Hevia, A. R. Kennedy, R. E. Mulvey, C. T. O'Hara, C. Talmard, *Angew. Chem. Int. Ed.* **2005**, *44*, 3459; *Angew. Chem.* **2005**, *117*, 3525; k) E. Hevia, G. W. Honeyman, A. R. Kennedy, R. E. Mulvey, D. C. Sherrington, *Angew. Chem. Int. Ed.* **2005**, *44*, 68; *Angew. Chem.* **2005**, *117*, 70; l) B. Conway, E. Hevia, A. R. Kennedy, R. E. Mulvey, *Chem. Commun.* **2007**, 2864; m) A. J. Martinez-Martinez, D. R. Armstrong, B. Conway, B. J. Fleming, J. Klett, A. R. Kennedy, R. E. Mulvey, S. D. Robertson, C. T. O'Hara, *Chem. Sci.* **2014**, *5*, 771; n) A. J. Martínez-Martínez, A. R. Kennedy, R. E. Mulvey, C. T. O'Hara, *Science* **2014**, *346*, 834.

[9] For reviews in the area, see: a) C. Alonso-Moreno, A. Antiñolo, F. Carrillo-Hermosilla, A. Otero, *Chem. Soc. Rev.* **2014**, *43*, 3406; b) W.-X. Zhang, L. Xu, Z. Xi, *Chem. Commun.* **2015**, *51*, 254; c) L. Xu, W.-X. Zhang, F. Xi, *Organometallics* **2015**, *34*, 1787.

[10] See, for example: a) R. G. S. Berlinck, A. E. Trindade-Silva, M. F. C. Santos, *Nat. Prod. Rep.* **2012**, *29*, 1382; b) D. Castagnolo, S. Schenone, M. Botta, *Chem. Rev.* **2011**, *111*, 5247; c) S. Ekelund, P. Nygren, R. Larsson, *Biochem. Pharmacol.* **2001**, *61*, 1183; d) P. P. Toth, *Postgrad. Med.* **2014**, *126*, 7; e) D. T. Nash, *J. Clin. Pharmacol.* **1973**, *13*, 416; f) N. Scheinfeld, *Dermatol. Online J.* **2003**, *9*, 4; g) M. von Itzstein, *Nat. Rev. Drug Discovery* **2007**, *6*, 967; h) Y. Hirata, I. Yanagisawa, Y. Ishii, S. Tsukamoto, N. Ito, Y. Isomura, M. Takeda, U. S. Patent **1981**, 4.283.408; i) E. Buchdunger, J. Zimmermann, H. Mett, T. Meyer, M. Mueller, B. J. Druker, N. B. Lydon, *Cancer Res.* **1996**, *56*, 100; j) L. Troncone, V. Rufini, *Anticancer Res.* **1997**, *17*, 1823; k) C. Loesberg, H. Van Rooij, J. C. Romijm, L. A. Smets, *Biochem. Pharmacol.* **1991**, *42*, 793.

[11] See, for example: a) P. J. Bailey, S. Pace, *Coord. Chem. Rev.* **2001**, *214*, 91; b) W. E. Piers, D. J. H. Emslie, *Coord. Chem. Rev.* **2002**, *233*, 131; c) M. P. Coles, *Dalton Trans.* **2006**, 985; d) P. C. Junk, M. L. Cole, *Chem. Commun.* **2007**, 1579; e) F. T. Edelmann, *Adv. Organomet. Chem.* **2008**, *57*, 183;

f) F. T. Edelmann, *Adv. Organomet. Chem.* **2013**, *61*, 55; g) J. Barker, M. Kilner, *Coord. Chem. Rev.* **1994**, *133*, 219; h) F. T. Edelmann, *Coord. Chem. Rev.* **1994**, *137*, 403; i) F. T. Edelmann, *Chem. Soc. Rev.* **2009**, *38*, 2253; j) F. T. Edelmann, *Chem. Soc. Rev.* **2012**, *41*, 7657; k) C. Jones, *Coord. Chem. Rev.* **2010**, *254*, 1273; l) A. A. Trifonov, *Coord. Chem. Rev.* **2010**, *254*, 1327.

[12] See, for example: a) T. Ishikawa, T. Isobe, *Chem. Eur. J.* **2002**, *8*, 552; b) T. Ishikawa, T. Kumamoto, *Synthesis* **2006**, 737; c) T. Ishikawa, *Superbases for Organic Synthesis: Guanidines, Amidines, Phosphazenes and Organocatalysts*, Wiley, New York, **2009**; d) J. E. Taylor, S. D. Bull, J. M. J. Williams, *Chem. Soc. Rev.* **2012**, *41*, 2109; e) D. Leow, C.-H. Tan, *Chem. Asian J.* **2009**, *4*, 488; f) P. Selig, *Synthesis* **2013**, 703; g) M. P. Coles, *Chem. Commun.* **2009**, 3659; h) X. Fu, C.-H. Tan, *Chem. Commun.* **2011**, *47*, 8210; i) A. Avila, R. Chinchilla, E. Gómez-Bengoa, C. Nájera, *Eur. J. Org. Chem.* **2013**, 5085; j) C. Thomasa, B. Bibal, *Green Chem.* **2014**, *16*, 1687.

[13] a) M. K. T. Tin, N. Thirupathi, G. P. A. Yap, D. S. Richeson, *J. Chem. Soc. Dalton Trans.* **1999**, 2947; b) M. K. T. Tin, G. P. A. Yap, D. S. Richeson, *Inorg. Chem.* **1998**, *37*, 6728; c) E. W. Thomas, E. E. Nishizawa, D. C. Zimmermann, D. J. Williams, *J. Med. Chem.* **1989**, *32*, 228.

[14] a) T.-G. Ong, G. P. A. Yap, D. S. Richeson, *J. Am. Chem. Soc.* **2003**, *125*, 8100; b) A. Grirrane, H. Garcia, E. Álvarez, *Beilstein J. Org. Chem.* **2013**, *9*, 1455; c) S. Zhou, S. Wang, G. Yang, Q. Li, L. Zhang, Z. Yao, Z. Zhou, H.-B. Song, *Organometallics* **2007**, *26*, 3755; d) F. Han, Q. Teng, Y. Zhang, Y. Wang, Q. Shen, *Inorg. Chem.* **2011**, *50*, 2634; e) L. Xu, Z. Wang, W.-X. Zhan, Z. Xi, *Inorg. Chem.* **2012**, *51*, 11941; f) J. Romero-Fernández, F. Carrillo-Hermosilla, A. Antiñolo, C. Alonso-Moreno, A. M. Rodríguez, I. López-Solera, A. Otero, *Dalton Trans.* **2010**, *39*, 6419; g) D. Elorriaga, F. Carrillo-Hermosilla, A. Antiñolo, F. J. Suárez, I. López-Solera, R. Fernández-Galán, E. Villaseñor, *Dalton Trans.* **2013**, *42*, 8223.

[15] T.-G. Ong, J. S. O'Brien, I. Korobkov, D. S. Richeson, *Organometallics* **2006**, *25*, 4728.

[16] a) C. Alonso-Moreno, F. Carrillo-Hermosilla, A. Garcés, A. Otero, I. López-Solera, A. M. Rodríguez, A. Antiñolo, *Organometallics* **2010**, *29*, 2789; b) D. Elorriaga, F. Carrillo-Hermosilla, A. Antiñolo, I. López-Solera, R. Fernández-Galán, A. Serrano, E. Villaseñor, *Eur. J. Inorg. Chem.* **2013**, 2940; c) A. Baishya, M. Kr. Barman, T. Peddarao, S. Nembenna, *J. Organomet. Chem.* **2014**, 769, 112; d) J. R. Lachs, A. G. M. Barrett, M. R. Crimmin, G. Kociok-Köhn, M. S. Hill, M. F. Mahon, P. A. Procopiou, *Eur. J. Inorg. Chem.* **2008**, 4173.

[17] To best of our knowledge, only three examples of magnesium complexes have been described so far in the literature as catalysts for guanylation reactions: Mg*n*Bu$_2$, [MgBz$_2$(THF)$_2$], and an *N*-heterocyclic carbene (NHC)-supported magnesium amide, see references [16a], [16b], and [16c], respectively.

[18] M. R. Crimmin, A. G. M. Barrett, M. S. Hill, P. B. Hitchcock, P. A. Procopiou, *Organometallics* **2008**, *27*, 497.

[19] S. E. Baillie, W. Clegg, P. Garcia-Alvarez, E. Hevia, A. R. Kennedy, J. Klett, L. Russo, *Chem. Commun.* **2011**, *47*, 388.

[20] a) X. Zhang, C. Wang, C. Qian, F. Han, F. Xu, Q. Shen, *Tetrahedron* **2011**, *67*, 8790; b) X. Zhu, Z. Du, F. Xu, Q. Shen, *J. Org. Chem.* **2009**, *74*, 6347.

[21] For other examples of structurally defined tris(amido)magnesiates, see: a) E. Hevia, F. R. Kenley, A. R. Kennedy, R. E. Mulvey, R. B. Rowlings, *Eur. J. Inorg. Chem.* **2003**, 3347; b) G. C. Forbes, A. R. Kennedy, R. E. Mulvey, P. J. A. Rodger, R. B. Rowlings, *J. Chem. Soc. Dalton Trans.* **2001**, 1477; c) W. Clegg, K. W. Henderson, R. E. Mulvey, P. A. O'Neil, *J. Chem. Soc. Dalton Trans.* **1994**, 769; d) B. J. Fleming, P. García-Álvarez, E. Keating, A. R. Kennedy, C. T. O'Hara, *Inorg. Chim. Acta* **2012**, *384*, 154; e) J. Francos, B. J. Fleming, P. García-Álvarez, A. R. Kennedy, K. Reilly, G. M. Robertson, S. D. Robertson, C. T. O'Hara, *Dalton Trans.* **2014**, *43*, 14424.

[22] D. Barr, W. Clegg, L. Cowton, L. Horsburgh, F. M. Mackenziec, R. E. Mulvey, *J. Chem. Soc. Chem. Commun.* **1995**, 891.

[23] X-ray analysis shows only three nonequivalent anilide fragments with *R*, *S*, *R*, *S* configuration for N4, N6, N2, and N1. However, during the identification of the hydrogen atoms on the Fourier map, a possible disorder was noticed that precludes the accurate establishment of the real configuration. Thus, two different possibilities can be found; a diastereomer with a configuration of the type *R*, *R*, *R*, *S*, which would show six inequivalent anilide fragments, or a mixture of diastereomers, such as *R*, *S*, *R*, *S* and *R*, *R*, *S*, *S*, which similarly would display a total of six signals for the anilide fragments.

[24] R. Neufeld, D. Stalke, *Chem. Sci.* **2015**, *6*, 3354.

[25] For examples of sodium magnesiates that display a SSIP structure in which sodium is solvated by THF molecules, see: a) D. R. Armstrong, W. Clegg, A. Hernan-Gomez, A. R. Kennedy, Z. Livingstone, S. D. Robertson, L. Russo, E. Hevia, *Dalton Trans.* **2014**, *43*, 4361; b) V. L. Blair, W. Clegg, A. R. Kennedy, Z. Livingstone, L. Russo, E. Hevia, *Angew. Chem. Int. Ed.* **2011**, *50*, 9857; *Angew. Chem.* **2011**, *123*, 10031.

[26] See the Supporting Information for synthesis and spectroscopic characterization.

[27] For other examples of structurally defined guanidinates where a similar rearrangement has taken place, see references [14g], [16a], [16d], and W. X. Zhang, M. Nishiura, Z. Hou, *Chem. Eur. J.* **2007**, *13*, 4037.

[28] G. J. Moxey, A. J. Blake, W. Lewis, D. L. Kays, *Eur. J. Inorg. Chem.* **2015**, 5892.

[29] A similar motif has been also reported by Chang for the reaction of Mg[N(*i*Pr)$_2$]$_2$ with two equivalents of DIC, see: B. Srinivas, C.-C. Chang, C.-H. Chen, M. Y. Chiang, I.-T. Chen, Y. Wang, G.-H. Lee, *J. Chem. Soc. Dalton Trans.* **1997**, 957.

[30] G. R. Giesbrecht, A. Shafir, J. Arnold, *J. Chem. Soc. Dalton Trans.* **1999**, 3601.

[31] C. N. Rowley, T.-G. Ong, J. Priem, T. K. Woo, D. S. Richeson, *Inorg. Chem.* **2008**, *47*, 9660.

[32] S. E. Baillie, W. Clegg, P. Garcıa-Álvarez, E. Hevia, A. R. Kennedy, J. Klett, L. Russo, *Organometallics* **2012**, *31*, 5131.

[33] For an example of anionic activation of magnesium reagents by forming mixed ammonium-magnesiate salts, see: C. Vidal, J. Garcia-Alvarez, A. Hernan-Gomez, A. R. Kennedy, E. Hevia, *Angew. Chem. Int. Ed.* **2014**, *53*, 5969; *Angew. Chem.* **2014**, *126*, 6079.

[34] A. Mukherjee, T. K. Sen, S. K. Mandal, B. Maity, D. Koley, *RSC Adv.* **2013**, *3*, 1255.

[35] J. H. Espenson, *Chemical kinetics and reaction mechanisms*, 2nd ed.; McGraw-Hill: New York, **1995**.

[36] J. F. Dunne, D. B. Fulton, A. Ellern, A. D. Sadow, *J. Am. Chem. Soc.* **2010**, *132*, 17680.

[37] J. Klett, W. Clegg, B. Conway, A. R. Kennedy, R. E. Mulvey, L. Russo, *Eur. J. Inorg. Chem.* **2011**, 721.

[38] a) Q. Li, S. Wang, S. Zhou, G. Yang, X. Zhu, Y. Liu, *J. Org. Chem.* **2007**, *72*, 6763; b) Z. Du, W. Li, X. Zhu, F. Xu, Q. Shen, *J. Org. Chem.* **2008**, *73*, 8966; c) M. P. Coles, P. B. Hitchcock, *Chem. Commun.* **2002**, 2794.

[39] *CrysAlisPro*; Oxford Diffraction: Oxford, *UK* **2008**.

[40] G. Sheldrick, *Acta Crystallogr. Sect. C* **2015**, *71*, 3–8.

Received: June 17, 2016
Published online on ■■ ■■, 0000

FULL PAPER

Cooperative Effects

M. De Tullio, A. Hernán-Gómez, Z. Livingstone, W. Clegg, A. R. Kennedy, R. W. Harrington, A. Antiñolo, A. Martínez, F. Carrillo-Hermosilla, E. Hevia**

■■ – ■■

Structural and Mechanistic Insights into s-Block Bimetallic Catalysis: Sodium Magnesiate-Catalyzed Guanylation of Amines

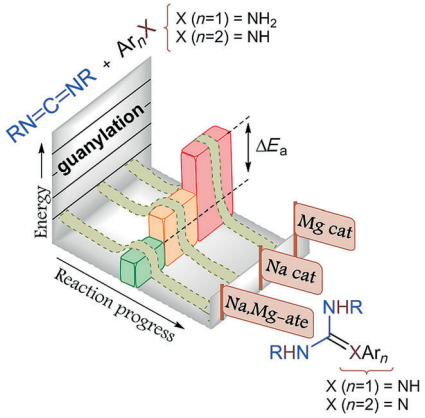

Magnesium activATES: Showing enhanced catalytic ability compared with their homometallic components (see figure), mixed Na/Mg complexes effectively catalyze the guanylation of a range of amines under mild reaction conditions, the key for which is the anionic activation of magnesium after installation within a sodium magnesiate platform.